lubricants

MDPI

Article

The Surface Assessment and the Properties of Selected Multilayer Coatings

Bogdan Warcholinski [1,*], Adam Gilewicz [1] and Maria Tarnowska [2]

[1] Faculty of Mechanical Engineering, Koszalin University of Technology, 75-453 Koszalin, Poland; adam.gilewicz@tu.koszalin.pl
[2] Centre for Biological Treatment, Independent Public Clinical Hospital No. 1, Pomeranian Medical University in Szczecin, 71-252 Szczecin, Poland; m.tarnowska@spsk1.szn.pl
* Correspondence: bogdan.warcholinski@tu.koszalin.pl

Abstract: The paper presents an evaluation of the surface quality and properties of multilayer coatings, obtained using cathodic arc evaporation, of the same structure, in which the top layer is a CrN chromium nitride layer. The second components of a double-layer module with a thickness of 400 nm and a thickness of each layer about 200 nm are two component TiN, Mo_2N systems and three component TiAlN and CrCN systems. In studies using scanning electron microscopy and optical microscopy, the surface density of the macroparticles of the coating and their dimensions were estimated. The largest amount of macroparticles was recorded on the surface of the TiAlN/CrN coatings and the lowest on CrCN/CrN and Mo_2N/CrN coatings. Their adhesion to steel substrates using a scratch test and Rockwell test and wear were also investigated. The results indicated that the melting point of the cathode material directly affected the number and size of the macroparticles on the surface of the growing coating. The number of macroparticles increased with the lowering of the melting point of the cathode material. All the coatings showed good adhesion with the critical load Lc_2, greater than 60 N with a hardness above 20 GPa. The Mo_2N/CrN coating, despite its relatively low critical load compared to the other tested coatings, had the best wear-resistant properties, which was probably due to the $Mo_2N \rightarrow MoO_3$ transformation.

Keywords: PVD; multilayer coatings; roughness; friction; wear

Citation: Warcholinski, B.; Gilewicz, A.; Tarnowska, M. The Surface Assessment and the Properties of Selected Multilayer Coatings. *Lubricants* **2023**, *11*, 371. https://doi.org/10.3390/lubricants11090371

Received: 8 August 2023
Revised: 28 August 2023
Accepted: 1 September 2023
Published: 3 September 2023

1. Introduction

Some of the transition metals (Ti, V, Cr, Zr, Nb, Mo, Ta, and W) are widely used for forming composite coatings of nitrides and carbides. They are characterized by good mechanical properties, mainly a high hardness, good adhesion, toughness, wear by friction, and temperature resistance, but also a high reactivity with mating material.

The world's growing population has caused a significant increase in the demand for wood and wood composites for various applications. This has caused an increase in the interest in high-performance wood-processing techniques, and mainly, the tools used in them. Among the most effective are tools those with thin, hard coatings that allow for working in dry conditions. Thus, in the case of wood, a hygroscopic material, its treatment can be carried out without cooling lubricants. Currently, many works are being carried out aimed at developing new coatings enabling the more effective processing of wood raw material [1,2].

The coatings of transition metal nitrides synthesized using PVD (Physical Vapor Deposition) exhibit properties that enable multiple applications. They allow for increasing tool life and improving their resistance to corrosion. Their use can reduce the consumption of coolants or eliminates them from the treatment of certain types of materials. Titanium nitride TiN coatings are characterized by a high hardness, but start to oxidize at a temperature of 550 °C [3]. Chromium nitride coatings are more resistant to oxidation compared to other

metal nitride coatings, and show a good wear resistance. Both coatings are characterized by a very good adhesion to substrates. A slightly worse adhesion is presented by CrCN [4] and Mo_2N [5] coatings.

The coatings formed using cathodic arc evaporation are characterized by a high hardness, good adhesion, high density, and homogeneity, and they show better properties than coatings prepared using magnetron sputtering. The disadvantage of this deposition method is the relatively high roughness of the coatings' surfaces, resulting from a large number of macroparticles on these surfaces. The number of macroparticles per unit area and their linear dimensions are dependent on the melting point of the cathode [6,7]. The studies of Creasy et al. [6] and Munz et al. [7] indicated that, as the melting point of a cathode increases the number of macroparticles, the maximum macroparticle size and fraction of sample area covered by macroparticles decrease. Harris et al. [8] investigated the effect of nitrogen pressure increase during the formation of TiN coatings on HSS (M2) jobber drills on the surface quality and efficiency of the drilling process. They showed that the coatings formed at a higher nitrogen pressure were characterized by a lower roughness and the number of macroparticles per unit area and maximum macroparticle diameter were significantly reduced, probably increasing the tool life.

Equally important as the selection of the method of formation of protective coatings (magnetron sputtering or cathodic arc evaporation) is the selection of the coating itself, including its type. Multilayer coatings generally have better properties than single-layer coatings. They have a greater hardness and adhesion to substrates, which often leads to a greater resistance to wear and corrosion. A modification of the structure of the coating [9,10] enables it to improve its functional properties. Multilayer coatings are characterized by an increased stability compared to monolayer coatings. This is due to their different mechanism of destruction [10,11], caused also by the interruption of the columnar growth of the coating. This may cause crack deflection, leading to a toughening of the coating in the interlayer zone, and may reduce stress concentration and crack propagation [11].

The properties of two-component coatings can be improved by changing their chemical composition—by doping metallic or non-metallic elements or modifying the structure of the coating—for example, reducing the grain size or forming a multilayer coating. The design of the multilayer coating can include the thickness of each layer, the chemical and phase composition, and its mechanical properties (hardness and Young's modulus) [8]. The coating used on tools should be characterized by a chemical inertness of the outer surface of the coating with processed material, a high hardness at the middle part of the coating, and a good adhesion to the substrate. A single-layer coating rarely meets all of these requirements. For example, an increase in hardness results in a reduction in coating ductility. A modification of the structure of a coating [9,10] enables it to improve its functional properties.

Santana et al. [12], examining the properties of TiAlN/CrN coatings, indicated the advantages of the use of a bilayer with a thickness of 400 nm and broad transition zones between the layers of the coating. These include increases in hardness and adhesion resulting from the interdiffusion of the layer components, due to a high energy ion bombardment, which is characteristic for arc coating processes. This reduces the mismatch of the lattice parameters of the crystal structures of the layers. Simultaneously, the temperature-activated diffusion process, with a larger thickness of modules, does not degrade the multilayer structure. In turn, Kot et al. [13], analyzing Cr/CrN multilayer coatings with thicknesses of (Cr + CrN) their bilayer from 62 to 1000 nm, found that, for the thickness of the bilayer from 250 to 500 nm, both the hardness, Young's modulus, and adhesion of the coating were the highest.

Due to their properties [14–16], chromium nitride coatings are widely used in many industrial applications [17–19]. The incorporation of Al into chromium nitride coatings improves their oxidation resistance at elevated temperatures (above 900 °C [20]) and their hardness, significantly increasing their durability. Such coatings are applied, for example, to woodworking tools [21–24].

TiAlN is characterized by a higher *temperature* resistance than *TiN*. TiAlN coatings oxidize at a temperature above 700 °C. The high wear of TiAlN coatings (higher than TiN coatings) operated at a low temperature results from their brittleness and high coefficient of friction. The main advantage of such a coating is its high-temperature stability. In TiAlN coatings "working" in an oxidizing environment at a temperature above 700 °C, a two-layer structure is formed. In the upper art of the aluminum-rich coating, a dense Al_2O_3 layer is formed, and in the inner part, a layer with a predominant titanium concentration. The top Al_2O_3 layer reduces diffusion wear during high-temperature machining and is renewed when the outer part of the coating is worn off. At a high temperature, chromium and aluminum oxides have lubricating properties. In addition, aluminum oxide acts as a diffusion barrier, blocking the diffusion of oxygen into the coating. The hardness of TiAlN coatings at a high temperature strongly depends on their chemical composition and is higher than that of TiN coatings [25,26].

It was found that the addition of chromium to TiAlN coatings improves their resistance to oxidation [27].

Molybdenum nitride coatings have excellent properties: a low wear rate and low coefficient of friction, combined with a high hardness and good adhesion, makes them a good candidate for tribological applications [28–30]. In an oxidizing environment and at an elevated temperature, molybdenum nitride oxidizes and MoO_3 is formed. This allows it to be used as a self-lubricating tribological coating operating at a high temperature [31].

There have been many studies on the properties of multi-layer coatings Me(X)N/CrN, where Me is a transition metal and X is an additional element, but few studies have included two-layer coatings with CrN as a topcoat. This is especially true for Mo_2N/CrN coatings, in which molybdenum has the ability to form oxides, known as solid lubricants, significantly reducing their wear. The small coefficient of friction of about 0.3–0.4, small compared to CrN (0.6) and TiAlN (0.8) coatings, and may be associated with the formation of MoO_3 in the friction process, characterized by favorable sliding properties. A similar effect, lowering the coefficient of friction, can be achieved by doping the coating with carbon. Hence, we attempt to compare the properties of Mo_2N/CrN and CrCN/CrN coatings.

The aim of the work was to check how the roughness of the multilayer coating changed:

(a) with the same CrN surface layer and a second layer formed from cathodes with different melting points: TiAl (approx. 1450 °C) and Mo (approx. 2650 °C),
(b) when both layers in the multilayer coating were formed from the same cathode (Cr) but one of the layers was doped with a non-metallic element, carbon.

It was also important to study the mechanical properties of these coatings and carry out industrial tests on tools covered with these coatings by planing dry pine in order to determine their suitability for this type of processing.

2. Materials and Methods

2.1. Coating Deposition

TiN, TiAlN, CrCN, Mo_2N, and CrN monolayer coatings, and related TiN/CrN and Mo_2N/CrN and TiAlN/CrN and CrCN/CrN multilayer coatings, were formed via cathodic arc evaporation using the TINA 900M device on silicon wafers (for stress measurements), HS6-5-2 steel substrates with a diameter of 32 mm (for mechanical tests), and planer knives made of the same steel, with dimensions of 160 × 30 × 3 mm, manufactured by Leitz GmbH & Co. KG, Oberkochen, Germany (for industrial testing). In this project, Ti (99.999%) $Ti_{30}Al_{70}$ (99.9%) Mo (99.98%), and Cr (99.999%) cathodes with a diameter of 100 mm and thickness of 12 mm were used. The substrates (hardness above 62 HRC) were ground and polished to a roughness parameter Ra of 0.02 μm, and then they were chemically degreased and ultrasonically cleaned in a hot alkaline bath for 10 min. After washing in distilled water and hot-air drying, the substrates were mounted on the rotating holder (2 rev/min) in a vacuum chamber at a distance of 18 cm from the arc sources. The chamber was evacuated to a pressure of 1×10^{-3} Pa. Prior to the deposition, the substrates were sputter cleaned at a nitrogen pressure of 0.5 Pa using argon and chromium ions

under a substrate bias voltage of −600 V for 10 min. Cr ion bombardment was used to remove contamination and the oxide layer from the surfaces of the substrates, enabling the good adhesion of the deposited coatings. A thin (about 0.1 μm) chromium layer was also deposited onto the substrate to improve its adhesion [32]. A deposition process was performed on substrates heated to a temperature of 300 °C, at a substrate bias voltage of −70 V, with the arc current and nitrogen pressure corresponding to each of the targets (Table 1). A CrCN coating was formed by introducing acetylene C_2H_2 (flow rate 10 sccm) to the vacuum chamber.

Table 1. The deposition parameters of the coatings.

	TiN	Mo_2N	CrN	TiAlN	CrCN
Nitrogen pressure [Pa]	0.5	1.8	1.8	1.0	1.8
Arc current [A]	80	140	80	60	80

Multilayer coatings were synthesized by alternating the deposition of monolayers from two sources placed on the opposite sides of the vacuum chamber. The thickness of the layer depended on the exposure time of the substrate in front of a given source, i.e., the rotational speed holder on which the substrate was placed. The multilayer coatings were composed of repeated bilayers with a constant thickness. One of the layers in each of the investigated multilayer coatings was a CrN layer. The coating thickness was controlled by the time of deposition. The basic parameters of the multilayer coatings' structures are summarized in Table 2.

Table 2. The structure of multilayer coatings.

	TiN/CrN	Mo_2N/CrN	TiAlN/CrN	CrCN/CrN
Coating thickness, (μm)	2.8	3.1	4.0	3.0
Number of bilayer	6	6	8	7
Bilayer thickness, (nm)	450	500	500	400
Thickness ratio of the layers in bilayer	1:1	1:1	1:1	1:1

2.2. Characterization

The microstructure and morphology of the coating surfaces were determined using a scanning electron microscope (JEOL JSM-5500LV). An analysis of the composition was completed using energy dispersive X-ray spectroscopy, EDS (Oxford Link ISIS 300).

The surface roughness of the coatings was evaluated with a Hommel Werke T8000 profilometer. The test was performed five times for each sample.

To define the size of the macroparticles and number of macroparticles on the unit of area on the surface of the coatings, the metallographic microscope Nikon Eclipse MA200 equipped with NIS-Elements software was used. The measurement area was about 133 × 171 μm^2. The surfaces of the coatings were recorded at the same magnification (400×), contrast, and sharpness. For each sample, five measurements in one line at equal distances from each other were carried out.

The coating thickness was determined using the ball-cratering method (Calotest), according to the EN 1071-2: 2002 European Standard.

The adhesion of the coatings was evaluated using a scratch test (Revetest Scratch Tester, CSEM) with a diamond indenter Rockwell C type with a 0.2 mm tip radius. The pre-defined parameters were: a scratch length of 10 mm, scratch speed of 10 mm/min, and normal load (100 N) progressively increasing at the speed of 100 N/min. The Lc_1 critical load was determined as the load at which the first cracks in the coating appeared, and the Lc_2 critical load as the load at which the total detachment of the coating from the substrate was observed. These loads were evaluated by observation using an optical

microscope as the average of at least three measurements. These results were verified using the Daimler-Benz test [33], which qualitatively evaluates the adhesion of coatings as a size and types of failure modes of the coating formed as a result of a Rockwell indentation force of about 1500 N.

For the hardness measurements, the nanohardness tester FISCHERSCOPE HM2000 equipped with a Berkovivh indenter was used. The hardness measurement of the coatings deposited using cathodic arc evaporation was difficult because of the large number of macroparticles on the surface, resulting in a high roughness. Thus, meeting the requirements for a correct measurement of hardness, so that the depth of the indentation did not exceed 1/10 of the total coating thickness (in order to eliminate the effect of the substrate) and the depth of the indentation was not less than 20 × Ra (arithmetic mean roughness), was difficult. Therefore, the method described by Romero et al. [34] was used. For this reason, the coatings were polished with fine diamond powder (1 µm) in order to remove these surface defects. After this operation, significantly reducing the surface roughness of the coatings, the statistic of the measurements was highly improved. In total, 20 measurements were made for each sample. At a fixed indenter penetration depth of 0.2 µm, using the device software (WIN-HCU software), the average value of the coating hardness and its Young's modulus, as well as measurement uncertainties, were obtained.

The stress of the coating was determined using the Stoney formula [35]:

$$\sigma = \frac{E}{1-\nu}\frac{t_s^2}{6t_f}\frac{1}{R} \quad (1)$$

Silicon wafers with a thickness of 0.3 mm, a length of 30 mm, and a width of 4 mm were used.

Studies carried out in the pin-on-disc system enable an estimation of the tribological properties of coatings, i.e., their coefficient of friction and wear rate. The parameters of the test were: a normal load of 20 N, sliding speed of about 0.2 m/s, distance of 1000 m, environment—dry friction in air at a temperature of 20 °C, and humidity of about 50%. Alumina balls with a diameter of 10 mm and roughness R_a of <0.03 µm were used as a counterpart. The wear rate was estimated as the wear volume (based on wear track profile—Hommel Werke T8000) divided by the normal load and the sliding distance [36].

Industrial tests were carried out using a Weinig H23 four-side planer machine equipped in 6 heads. The working parameters were: cutting speed—50 m/s, spindle speed—6000 min^{-1}, feed rate—73 m/min, and cutting depth—1 mm. The machined material was overdried pine wood. Under these conditions, industrial tests were carried out for 8 h. Their purpose was not to determine the actual increase in durability, but to evaluate the rake face of knives modified with the investigated coatings in the same time and under the same working conditions of the tools.

3. Results

3.1. Chemical Composition of the Coatings

The chemical composition of the investigated coatings is presented in Table 3. This composition applies to the entire coatings, not the individual layers.

3.2. Surface Morphology

The images of the PVD (Figure 1) coatings' surfaces revealed a large number of defects, macroparticles, or pinholes formed when removed, or as a shadow effect when it was applied. These defects resulted in an increase in the surface roughness of the coating and worsening of its quality. This is a negative phenomenon that is the subject of relatively few works [6,7,37,38].

Table 3. The chemical composition of the coatings (at.%).

	TiAlN/CrN	Mo_2N/CrN	CrCN/CrN
Ti	13.8	-	-
Al	25.7	-	-
Mo	-	29	-
Cr	6.8	23.5	50.2
C	-	-	4.9
N	53.7	47.5	44.9

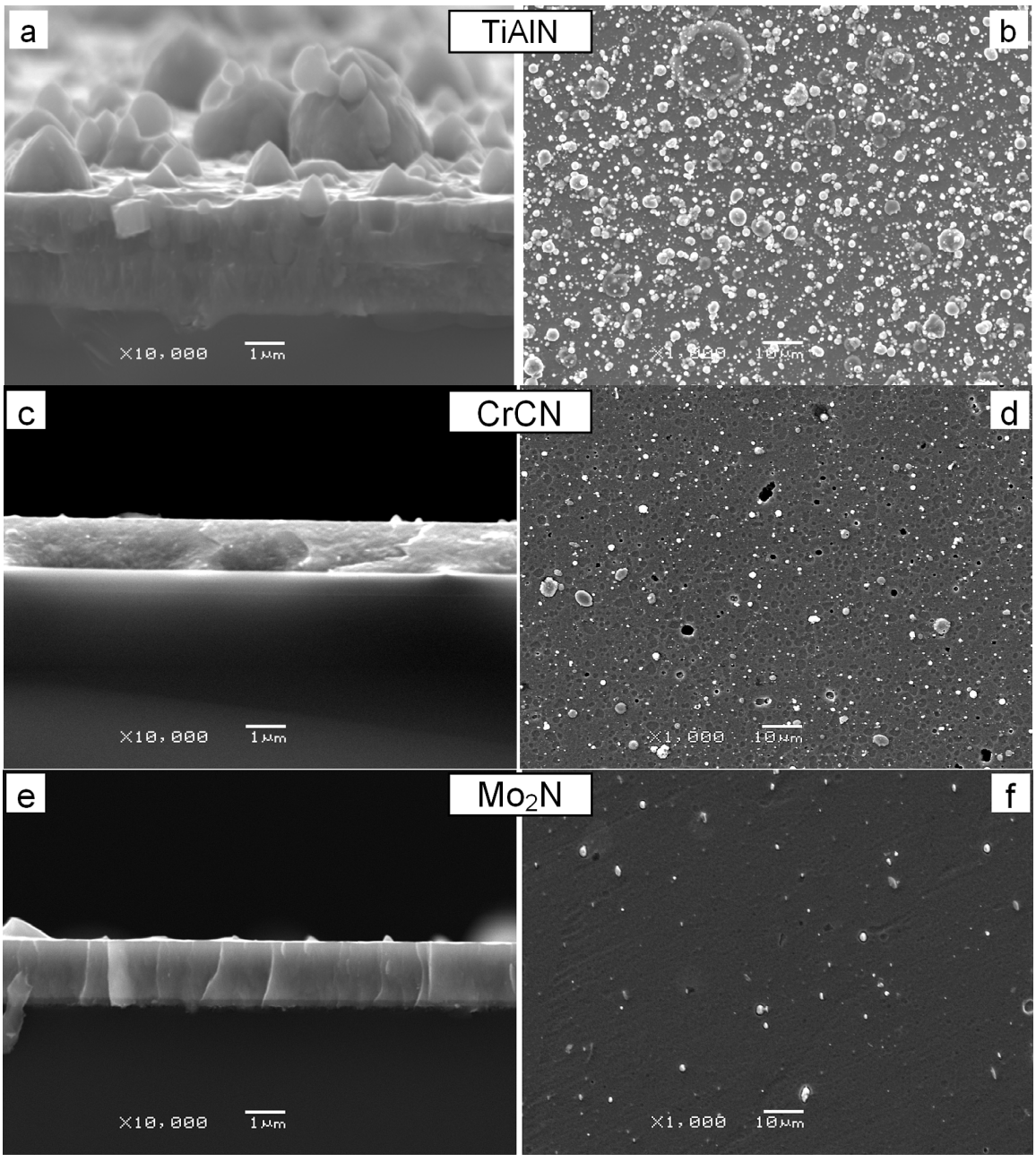

Figure 1. *Cont.*

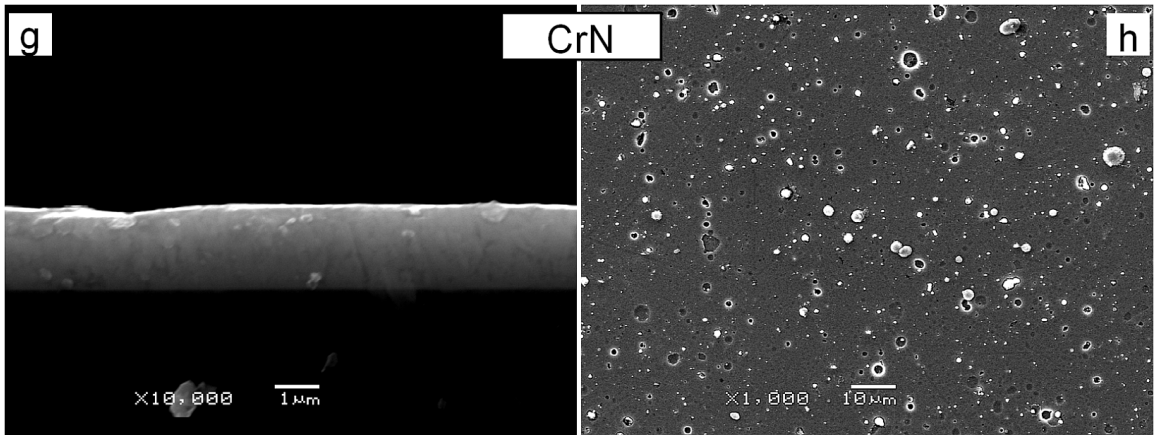

Figure 1. Images of cross-sections (**a**,**c**,**e**,**g**) and surface (**b**,**d**,**f**,**h**) of TiAlN (**a**,**b**), CrCN (**c**,**d**), Mo_2N (**e**,**f**), and CrN (**g**,**h**) monolayer coatings.

The top layer of the all the multilayer coatings investigated was a chromium nitride layer. Despite this, the amount of macroparticles on the coating surfaces varied. This was shown in two multilayer coatings: TiAlN/CrN and CrCN/CrN—Figure 2. The multilayer coating structure is clearly marked. The column growth was significantly limited, although possible.

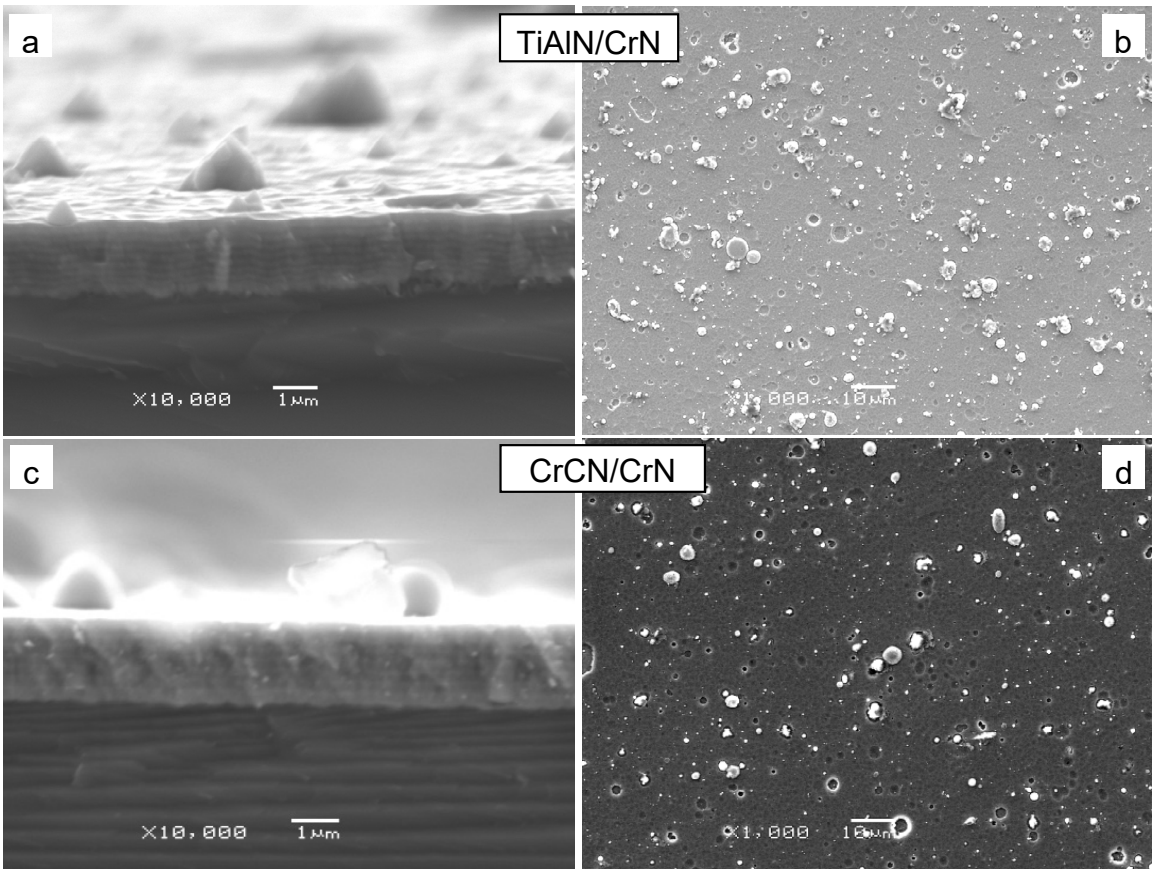

Figure 2. Images of cross-sections (**a**,**c**) and surface (**b**,**d**) of TiAlN/CrN (**a**,**b**) and CrCN/CrN (**c**,**d**) multilayer coatings.

In the cathodic arc evaporation method, the plasma jet contains not only electrons, ions, and atoms, but also droplets of the molten metal of the cathode. They are the biggest

disadvantage of the arc method. Droplets of different sizes are deposited on the substrate. One can observe only a small part of them on the surface. Some of them extend from the substrate to the coating surface. Smaller droplets with spherical shapes and larger, more irregular droplets are often "anchored" in the coating.

3.3. Macroparticle Statistics

The measurement of the size and quantity of the macroparticles on the surface of the coating was performed at the same area of about 133 × 171 μm^2 at five randomly selected points. The number of registered particles and also the fraction of the sample area covered by the macroparticles, as well as the surface roughness Ra of the coating, are presented in Table 4.

Table 4. The number of macroparticles and fraction of sample area covered by macroparticles on investigated multilayer coatings formed using cathodic arc evaporation.

Type of the Coating	TiN/CrN	Mo_2N/CrN	TiAlN/CrN	CrCN/CrN
Area (μm^2)	2.27 × 10^4	2.27 × 10^4	2.27 × 10^4	2.27 × 10^4
Number of macroparticles	1281 ± 120	677 ± 40	3844 ± 720	612 ± 210
Fraction of sample area covered by macroparticles	15 ± 1	3 ± 1	41 ± 7	2.6 ± 0.9
Roughness Ra (μm)	0.20	0.09	0.32	0.08

Although the top layer of each multilayer coating was a CrN layer, one could observe very variable quantities of the macroparticles on their surfaces. The smallest amount (about 600–700 macroparticles) was observed on the CrCN/CrN and Mo_2N/CrN coatings, while much more was registered for the TiAlN/CrN coating. A large scatter of the fraction of the sample area covered by macroparticles was also found. For the Mo_2N/CrN and CrCN/CrN coatings, it was about 3%, while for the TiAlN/CrN coatings, it was more than 40%. These results correlated completely with the observations arising from Figures 1 and 2. Similar results were obtained by Wan et al. [37] for CrN coatings deposited using ion plating.

A dimension analysis of the macroparticles on the surfaces of the coatings tested indicated that about 80% of the objects were sized to 1.5 μm. The second-largest group of objects, about 10%, had dimensions in the range from 1.5 to 3.0 μm. It was interesting that part of each of the size fractions was similar for each of the coatings, regardless of their chemical composition—Figure 3.

A detailed analysis of the size distribution of the macroparticles was performed for two multilayer coatings: TiN/CrN and CrCN/CrN—Figure 4. The TiN/CrN multilayer coating had almost a two times greater macroparticles surface density compared to the more complex CrCN/CrN coating, while the dimensional distribution of the macroparticles in both coatings was similar. This may have been associated with the lower melting point of the titanium cathode (1660 °C) compared to the chromium cathode (1870 °C).

In multilayer coatings, their surface quality (e.g., expressed by the roughness parameter Ra) depends on the process conditions for the coating deposition of various cathodes and the kind of cathodes used. An analysis of the surfaces of the CrN and CrCN monolayer coatings [38] revealed that they had a surface roughness Ra, respectively, of (0.06 ± 0.01) μm and (0.10 ± 0.02) μm, and the CrCN/CrN multilayer coating had an intermediate value of Ra (0.08 ± 0.01) μm. Otherwise, it was with the Mo_2N/CrN multilayer coating, characterized by a roughness (Ra about 0,09 μm) higher than the coating component: Mo_2N, with a Ra about 0.04 μm [5]) and CrN, with a Ra about 0.06 μm [38].

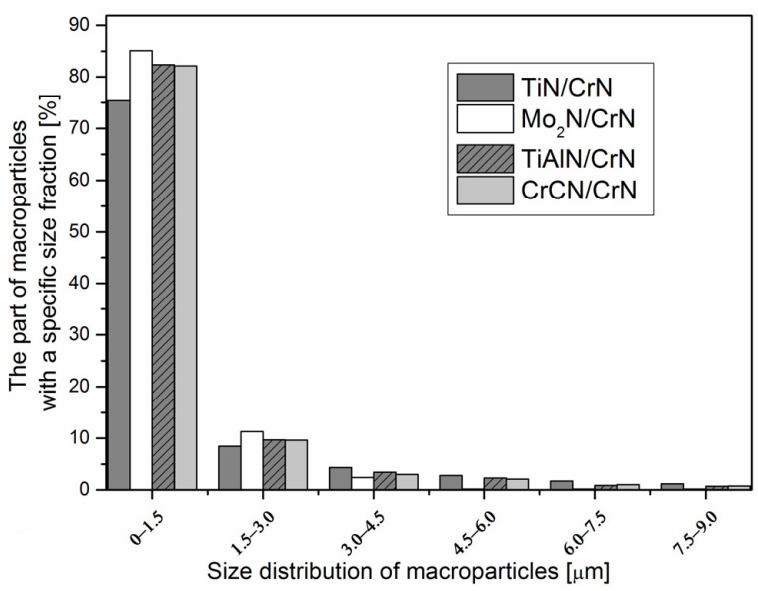

Figure 3. Part of macroparticles on the surface of multilayer coatings formed by cathodic arc evaporation, depending on the size distribution of macroparticles.

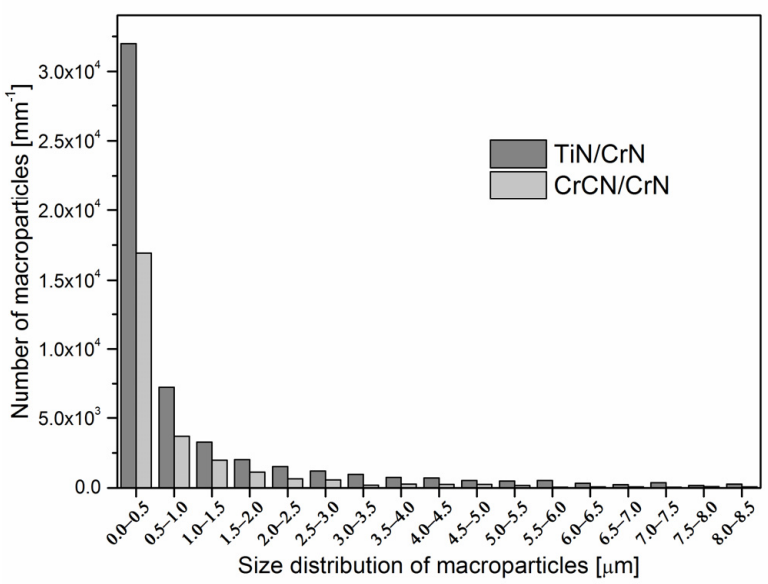

Figure 4. Size distribution of the macroparticles for TiN/CrN and CrCN/CrN multilayer coatings.

Surface roughness is defined as its irregularity associated with the occurrence of height and valleys in relation to a specific mean line. In many tribological applications, the maximum irregularity heights above the mean line are an important parameter, since they may damage the contact surfaces of the friction bodies. However, in the case of lubrication in the cavities, a lubricant reducing the friction between rubbing bodies may accumulate. Rough surfaces usually wear more quickly and have higher friction coefficients than smooth surfaces.

The surface roughness of coatings can be regulated by an arc current—Figure 5, but it should be remembered that a reduction in the arc current decreases the deposition rate of the coating, which increases the time of the deposition process.

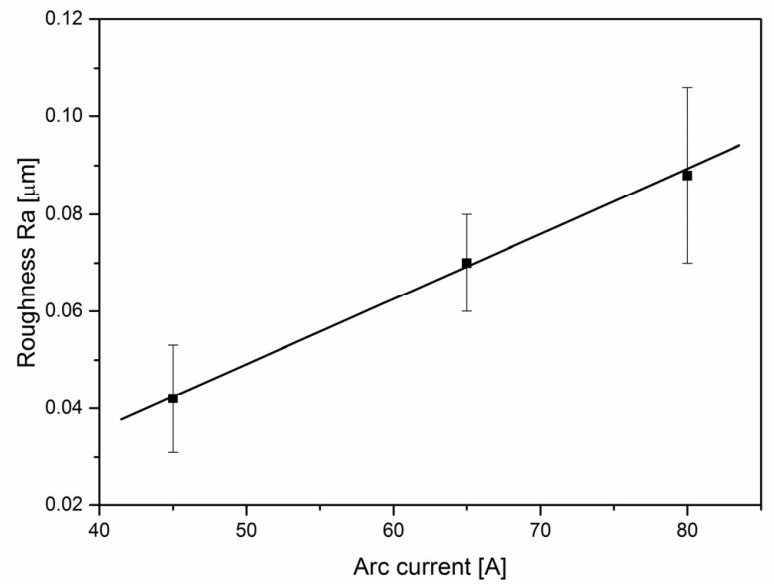

Figure 5. The relationship between surface roughness Ra of CrN monolayer coating obtained by cathodic arc evaporated depending to the arc current.

3.4. Hardness

The hardness of the coatings and other properties are summarized in Table 5. It should be noted that the hardness of TiAlN/CrN (21 ± 1 GPa) was lower than described in the literature [27,39–41], however, the thickness of the (TiAlN + CrN) bilayer was much smaller, at less than 50 nm. The hardness of the CrCN/CrN coating (24 ± 2 GPa) was higher than the hardness of both the chromium nitride (18 GPa) and chromium carbonitride (22 GPa). The Mo_2N/CrN coatings' hardness was comparable with Ref. [42].

Table 5. The mechanical properties of TiAlN/CrN, CrCN/CrN, and Mo_2N/CrN multilayer coatings.

Type of the Coating	TiAlN/CrN	CrCN/CrN	Mo_2N/CrN
Hardness H (GPa)	21 ± 1	24 ± 2	26 ± 2
Stress (GPa)	−1.0 ± 0.1	−1.5 ± 0.1	−1.1 ± 0.1
Young modulus E (GPa)	291 ± 15	258 ± 9	310 ± 12
H/E	0.072 ± 0.007	0.093 ± 0.011	0.085 ± 0.010
H^3/E^2 (GPa)	0.11 ± 0.03	0.21 ± 0.07	0.18 ± 0.06
Critical load Lc_2 (N)	82 ± 3	105 ± 2	59 ± 4
Coefficient of friction	0.72 ± 0.04	0.58 ± 0.04	0.40 ± 0.02
Wear rate of the coating ($mm^3N^{-1}m^{-1}$)	$(2.5 \pm 0.2) \times 10^{-7}$	$(1.3 \pm 0.6) \times 10^{-7}$	$(9.0 \pm 0.6) \times 10^{-8}$

3.5. Adhesion

The multilayer coatings discussed were characterized by a good adhesion to the substrate, Figure 6. This amounted to 59 N for the Mo_2N/CrN coating, 82 N for the TiAlN/CrN coating, and about 105 N for the CrCN/CrN coating. These values are close to those presented in the literature, although some single-layer coatings have a lower critical load [18,28,43,44].

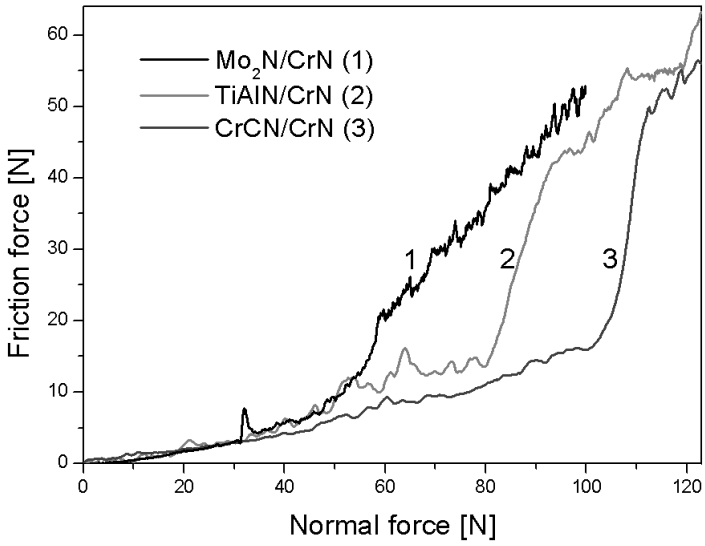

Figure 6. The friction force versus normal force in scratch test for coatings investigated.

Optical micrographs of the scratch section for the coatings tested at three loads are shown in Figure 7. The first is where the first coating failure was observed (Lc_1), the second shows the detachment of the coating from the substrate occurring (Lc_2), and the third is for an intermediate load. A relatively large critical force Lc_1 of the investigated coatings and a large difference between the loads Lc_1 and Lc_2 should be noted. This indicates a considerable resistance to the destruction of the coating. In the image of the crack formed after applying a load greater than Lc_1, there are numerous coating chips at the scratch border. This cracking of the coating and its partial delamination were related to the plastic deformation of the substrate and resulted from the different mechanical properties (hardness and Young's modulus) of the coating and the substrate.

In the scratch track, fine conformal hemispherical cracks perpendicular to the scratch direction are visible, indicating the high hardness and high adhesion of the coating. Minor chipping and cracking of the coating did not adversely affect its good properties. In the pictures of the scratches loaded by Lc_2, there are significant areas of coating losses.

The Daimler-Benz test is easy to apply, competent, and reliable, due to the large force applied indentation in the coating evaluation method for its adhesion and mechanisms for its destruction. The test allows for a visual assessment of the adhesion and durability of hard coatings. As the adhesion depends on the film thickness, hardness, and roughness of the substrate, a coating thickness of about 3–4 μm was used.

The Mo_2N/CrN coating adhesion test results are shown in Figure 8. Both distinct and circumferential and radial cracks are visible. Due to the pill-up of the substrate material around the indentation, there existed a high level of tensile stress. For brittle and hard materials, these stresses cause the formation of large circular cracks on the circumference of indentation [32].

In the TiAlN/CrN and CrCN/CrN coatings, probably due to their slightly lower hardness, only radial cracks occurred, which are frequent in the case of brittle coatings showing a good adhesion. In the TiAlN/CrN coatings, angular intersecting cracks also appeared, which may have contributed to an easier detachment of the coating from the substrate, as shown in Figure 8. The coatings tested were characterized by a good adhesion and they belonged to the group of HF1.

The results of the Daimler-Benz test and scratch test were comparable and showed that, among the tested coatings, Mo_2N/CrN showed a poorer adhesion.

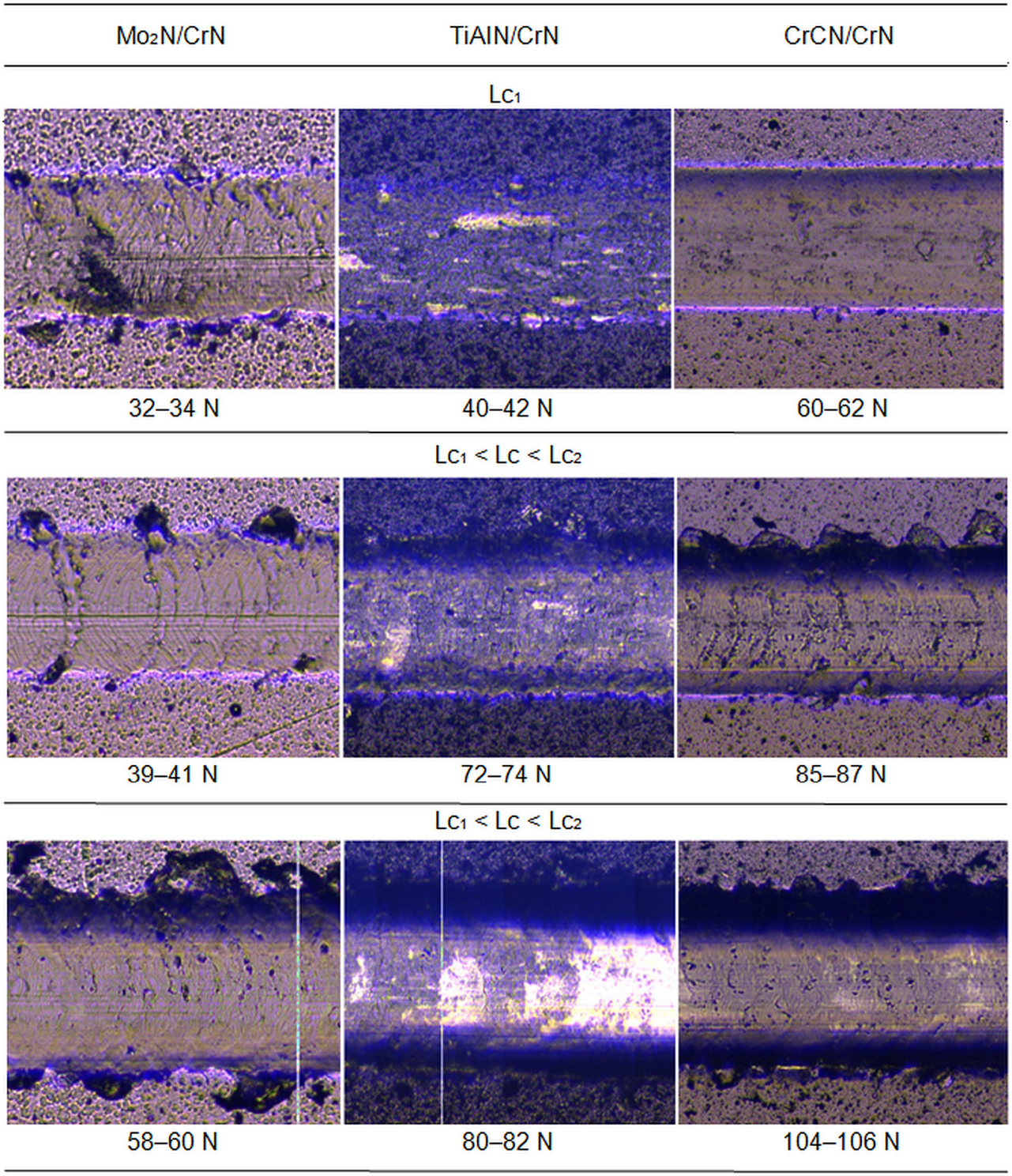

Figure 7. The scratch test and optical micrographs of failures at the critical load Lc_1, $Lc_1 < Lc < Lc_2$, and Lc_2 for coatings investigated.

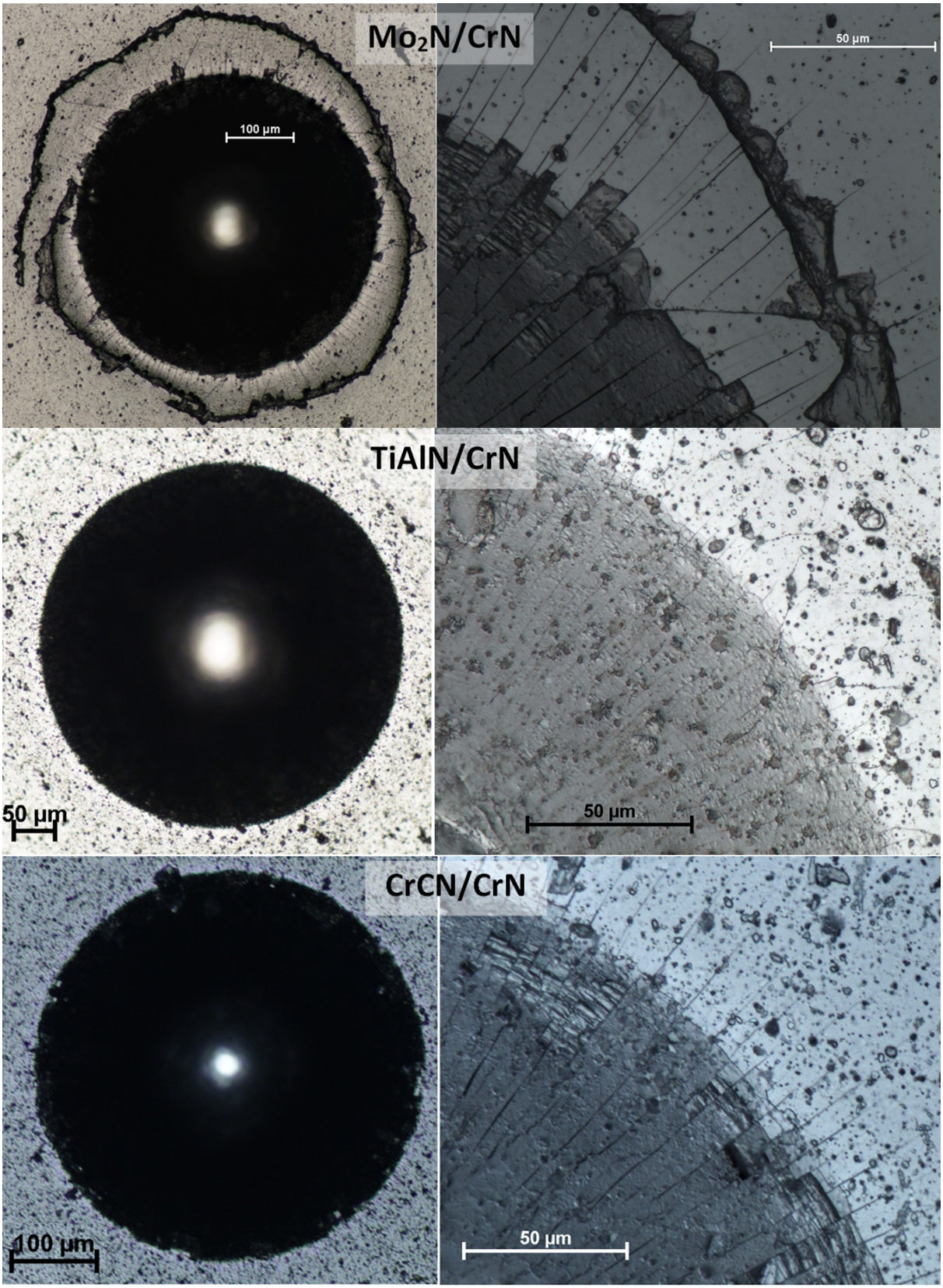

Figure 8. The picture of a Rockwell indentation in Mo_2N/CrN, TiAlN/CrN, and CrCN/CrN multilayer coatings.

3.6. Wear

The chromium addition to the TiAlN coating significantly reduced the wear rate, and for the TiAlN/CrN multilayer coating, it was about 30 times smaller (2.5×10^{-7} mm^3/Nm) compared to that of the TiAlN coating (7.8×10^{-6} mm^3/Nm). It is interesting that CrCN/CrN coating was characterized by an almost two times lower wear rate (1.3×10^{-7} mm^3/Nm), and that of the Mo_2N/CrN coating was even lower—9×10^{-8} mm^3/Nm. It should be noted that the test of friction for all the coatings was carried out under identical conditions. The results of the coefficient of friction are presented in Table 4. They corresponded to the coating wear rates. The highest was for the TiAlN/CrN coating (0.72) and the lowest for Mo_2N/CrN (0.4), which is similar to that presented in Refs. [39,41,45].

The real test of the wear of coatings dedicated to woodworking tools is an industrial test. Due to the anisotropy of the physical properties and anomalies in wood structures, as well as the use of high cutting speeds (to 100 m/s) and feed rate (20 ÷ 40 m/min), this test is more reliable than the laboratory test with a low sliding speed and normal load. The above values are much higher than those for metal machining, respectively—to 2 m/s and to 1 m/min. The cooling of the tool and workpiece used in metal processing is not possible with woodworking, therefore, the temperature of the tool is higher, which contributes to more severe test conditions and increased tool wear. The photographs of the cutting edge and rake face of the steel (HS6-5-2) knives with the coatings tested are shown in Figure 9.

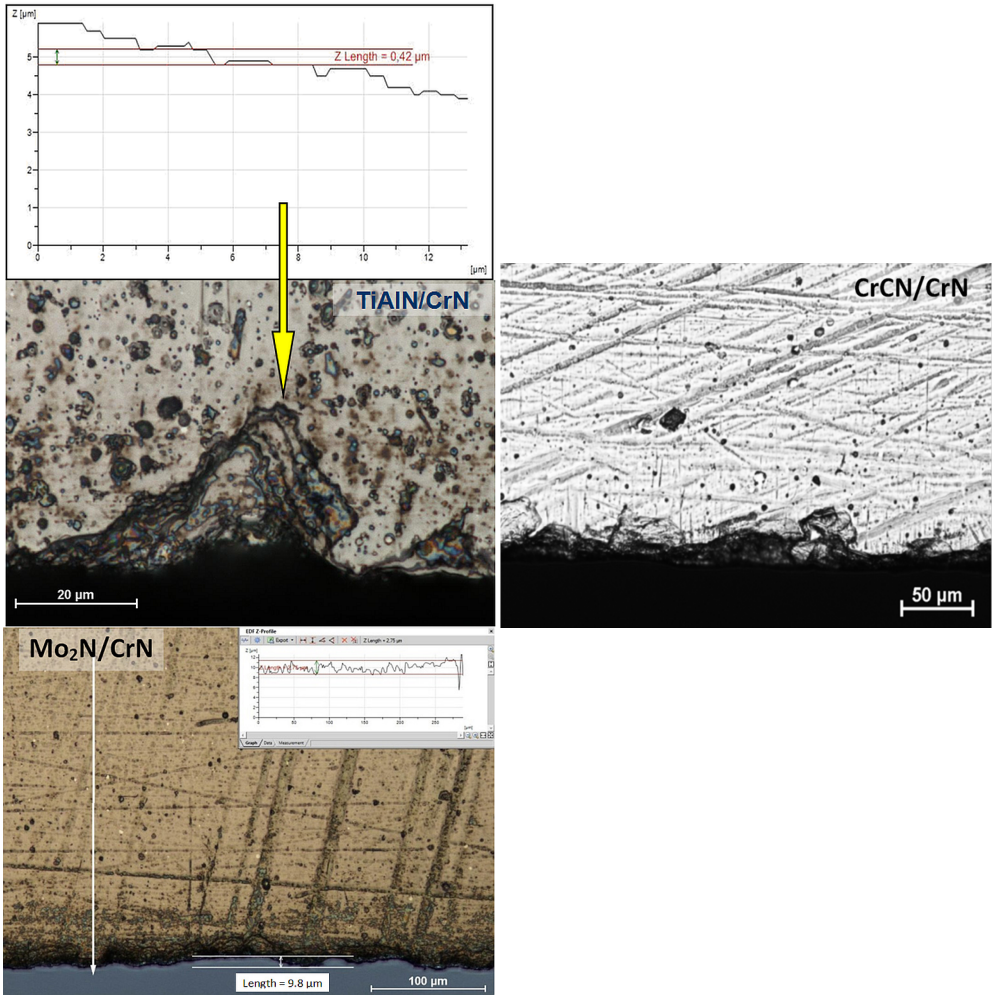

Figure 9. The images of the cutting edge and rake face of the planer knife made from HS6-5-2 steel with TiAlN/CrN, CrCN/CrN, and Mo_2N/CrN multilayer coatings.

On the edge of a planer knife coated with TiAlN/CrN, the chipping of the coating with a thickness of about 420 nm was observed. It corresponded to the thickness of the coating bilayer. The yellow arrow in Figure 9 indicates the direction of the profiling of the tool surface, perpendicular to the edge of the blade. For other coatings, there were only a few small chippings. The surface profile of the Mo_2N/CrN coating in the direction perpendicular to the surface of the blade edge, marked with a white arrow, is shown in the upper right part of the figure. It shows no significant abrasive wear.

The presented coatings were characterized by a good adhesion and they significantly improved the tool life. They exhibited an abrasive nature of wear, which meant that the temperature during machining did not exceed the tempering temperature of the blade material.

The wear of coatings is a complex process, in which one should take into account a number of possible changes in the chemical, physical, and mechanical properties both in the coating and interface of the coating–substrate. For this reason, the wear should be considered as a random process.

4. Discussion

The arc process of coating deposition is characterized by a high average kinetic energy of particles and a high degree of ionization of plasma. Almost all the particles (ions and atoms) and drops leaving around the cathode space reach the substrate. Hence, it follows a high deposition rate. The substrate bias voltage increases the energy of the particles and the substrate bombardment of high-energy particles results in the removal of macroparticles weakly bound to the substrate. A similar dimensional distribution for CrN monolayer coatings formed via cathodic arc evaporation was previously presented [38].

The disadvantage of TiAlN (Figure 1) coatings is their relatively high surface roughness, resulting from the low melting point of the TiAl cathode. The studies conducted by Munz et al. [6,7] suggested that, as the melting point of the cathode material increases, the amount of macroparticles of the cathode material deposited on a steel substrate decreases. Another negative feature is the decrease in the deposition rate as a result of the "target poisoning". In the case of TiAl cathodes with a relatively low melting point (about 1400–1500 °C, depending on the concentration of aluminum), it is particularly important because of the high melting points of TiN and TiAlN (about 3000 °C). The melting points of chromium and molybdenum amount to about 1900 °C and 2620 °C, respectively. The images of the surfaces of the TiAlN, CrCN, Mo_2N, and CrN coatings, deposited using cathodic arc evaporation, indicated a large amount of macroparticles on the TiAlN coating surface, less on the surfaces of the CrCN and CrN coatings, and an especially small amount on the surface of the Mo_2N coating, Figure 1.

The test results confirmed that the melting point of the cathode material had a large impact on the number of defects on the surface of the formed coating. The top layer of each tested multilayer coating was CrN. In spite of this fact, a significant difference was observed in the number of surface defects (Figure 2) or the roughness of the tested coatings, Table 4. The type of the second layer of the multilayer coating played an important role here. This was particularly evident in the case of the TiN/CrN and TiAlN/CrN coatings. In the former, the melting point of the cathode (1660 °C) was higher than that for the TiAl cathode, which directly translated into their roughness parameters Ra of 0.20 µm and 0.32 µm, respectively.

The chemical composition of the TiAlN/CrN coating was somewhat surprising, in fact, the Ti/(Ti + Al) ratio was about 0.35, which is more than that of the titanium concentration in the $Ti_{30}Al_{70}$ cathode. This was probably related to the resputtering effect of the deposited coatings and lower atomic weight of Al. This lower mass caused a greater scattering of the Al ions in collisions with nitrogen, which led to a lower vapor density and fewer of them reaching the substrate.

The hardness of the CrCN/CrN and Mo_2N/CrN coatings was close to the literature data, while the hardness of the TiAlN/CrN coating was slightly lower. This may have been due to the high concentration of aluminum in the coating, which reduced its hardness.

The wear of coatings can be considered in many areas. Often, the hardness property is considered to be decisive for their resistance to wear [46]. It is preferable, from the viewpoint of stability, to use the H/E ratio as an indicator of the durability of the coating, because this parameter generally is related to the ability of the elastic deformation of the coating material. The better adaptation of the elastic properties of the coating and substrate can improve its ability to adapt to the deformation of the substrate. The H/E ratio is a more important factor for wear resistance than high hardness. When considering the wear of the coating, the ability to deform both the substrate and the coated substrate and the ability to absorb deformation energy should be taken into account. A higher value for the H/E rate is a strong indication of the resistance to plastic deformation of the coating, but it does not always improve the ability of elastic deformation and fracture toughness. Both a high hardness of the coating and/or a low Young's modulus should cause a decrease in the effect of the deformation of the coating (and substrate) during scratch tests, reducing the coefficient of friction. The initiation of cracks in brittle material occurs with a lower energy than plastic material. When designing coatings, one should pay attention to the H/E ratio, because above a certain characteristic material value, its wear rate increases. For a lower wear, the ratio of the coating destruction mechanism changes from a brittle-to-ductile. A decrease in the H/E ratio due to a hardness decrease or Young's modulus increase results in the lowering of the coating's resistance to dynamic loads, and the coating becomes more plastic. For coatings with a low H/E (plastic materials), even low loads cause their strain and a rapid increase in stress, often exceeding the local strength. This results in the creation and propagation of microcracks that connect and lead to local delamination.

The H/E ratio was the lowest for the TiAlN/CrN coating and the highest for CrCN/CrN coating. The Mo_2N/CrN coating was characterized by a slightly lower value for the H/E ratio. It should be noted, however, that taking into account both the H/E value and measurement uncertainty, the CrCN/CrN and Mo_2N/CrN coatings had comparable values of this parameter. The same applied to their resistance to plastic deformation, i.e., the H^3/E^2 ratio. It was the lowest for the TiAlN/CrN coating, and comparable (within the limits of measurement uncertainty) for the other tested coatings. It should be noted that the roughness of the TiAlN/CrN coating was significantly higher than that of the other coatings, Table 4. The H/E and H^3/E^2 rates indicated the TiAlN/CrN coating as a coating with a lower wear resistance, and these were also the results of the wear measurement under laboratory tests, Table 5.

Significant effects on the wear are played by the surface conditions, its roughness, and the number of macroparticles on the surface of the coating. Macroparticles, in most cases, are the droplets of cathode material. They are soft in relation to the hardness of the coating and weakly bonded to it, and they can create a lubricating effect by grinding on the surface of the machined metal. However, even the small efficiency of a chemical reaction (e.g., nitridation) in the macroparticle sphere can cause their considerable hardening. Such detached particles can serve as an effective abrasive material, resulting in the faster processing of the material, but also accelerate the wear of the coating itself. Simultaneously, probably due to its hardness, a significant change in the dimension or degradation of the macroparticles does not occur. The fragmentation of the particles depends on their resistance to fracture toughness, and the higher the hardness, the higher the fracture toughness. Thus, the amount of macroparticles on the surface coating can be related to the wear of the coating during a friction test. In the case of the TiAlN/CrN coating, the number of macroparticles was the largest (also roughness parameter Ra); hence, the greater the wear rate of this coating. In the case of the CrCN/CrN and Mo_2N/CrN coatings, their quantities of macroparticles were similar (the roughness parameter Ra also) and wear rates were similar, although for the Mo_2N/CrN coating, these were slightly smaller.

The relatively low coefficient of friction of the CrN and Mo_2N coatings, Table 5, compared to TiN-based coatings, has also been the subject of many studies [47,48]. The physical and chemical processes occurring on the rubbing material surface favor a change in their chemical composition and phase. Metal oxides formed on the surface of the coating usually reduce the coefficient of friction and temperature in the frictional contact, and, consequently, reduce the wear of the coating [49]. Based on our previous research, we can conclude that, in the friction track of the CrCN coatings tested in laboratory conditions (normal force 20 N, sliding speed 0.2 m/s, and dry friction), an increased oxygen concentration is present [44]. The same effect was found in AlCrSiN coatings tested under the same conditions [50] and others.

It is known that the kind of wear products forming during friction determines the tribological behavior [51]. In particular, the chemical nature of the products formed during friction tests, i.e., the type of compound: simple, complex, and stoichiometry, has a significant effect on the phenomena taking place in the frictional contact. One of the theoretical approximations explaining the relationship between the chemistry of the friction products and lubrication is the approach proposed by Erdemir [49,52]. In this approach, the ionic potential plays an important role. Oxides or mixtures of metal oxides with a higher ionic potential φ, defined as the ratio of cation charge to the cation ionic radius, can decrease the coefficient of friction of the rubbing surfaces. A significant decrease in the coefficient of friction is observed for mixtures of oxides, in which the ionic potential difference is large.

The presence in friction pairs of oxides with a low ionic potential results in higher friction forces, which usually results in a higher wear. Metal oxides with a high ionic potential easily deform or are subjected to shear during friction. They are often called lubricious oxides. The test results of the products after the friction test carried out at room temperature revealed the existence of oxides produced by tribochemical reactions [48]. The ionic potentials of Cr_2O_3, CrO_2, TiO_2, Al_2O_3, MoO_3 were 4.0, 7.3, 5.8, 6.0, and 8.2, respectively [49]. The potential difference in ionic TiO_2 and Al_2O_3 is close to zero, which can result in a high coefficient of friction and wear, which is consistent with the approach proposed by Erdemir.

The Mo_2N/CrN coating case is a good example for considerations of wear. It was characterized by the smallest adhesion to the substrate, but also the highest wear resistance of the coatings tested. Because of the possibility of the formation of an oxide lubricious coating, for treatment without the use of coolants (elevated temperature), this coating can constitute an alternative to coatings based on TiAlN. In the Mo_2N/CrN coating at an elevated temperature (about 400 °C [53] or 680 °C [54]), Mo_2N transformed into MoO_3 molybdenum oxide via the reaction of [54]:

$$Mo_2N + 2O_2 = 2MoO_2 + \frac{1}{2}N_2 \quad (2)$$

$$MoO_2 + \frac{1}{2}O_2 = MoO_3 \quad (3)$$

Molybdenum oxide is characterized by a relatively low coefficient of friction [54]. The formation of oxides on the surface of the Mo_2N coating during friction is useful and can lead to a reduction in the coating wear. An abraded oxide surface layer is reproduced in the presence of oxygen in air. Even at room temperature, in wear products of Mo_2N coatings, the Raman spectroscopy reveals the presence of molybdenum oxide [48]. Such a mechanism of surface oxidation and the abrasion of the surface oxide layer have been described by Zhu [55].

CrN coatings are resistant to oxidation to about 800 °C, and MoN is likely to oxidize at about 500 °C [45]. The nano-layered structure of Mo_2N/CrN should be hard and lubricious at an elevated temperature. Chromium nitride CrN is a barrier against oxygen diffusion into the inner part of the coating and protects against the oxidation of the all the coating. Therefore, the inner Mo_2N layers of the multilayer coating do not oxidize, which, in view

of a layered structure of molybdenum oxide MoO_3 with weak van der Waals bonds, could lead to a rapid degradation of the coating under load.

Industrial tests showed that the greatest abrasive wear, as well as the local chipping of the coating, occurred in the TiAlN/CrN coating. Despite the registered high adhesion, the cohesion of the coatings was weaker, which was observed by the local layered chipping of the coating, as shown in Figure 9. The other coatings showed only slight abrasive wear with a slight chipping of the coating on the edge of the blade. A correlation of the wear results in the laboratory and industrial tests was observed. These results confirmed the applicability of the wear prediction H/E and H^3/E^2 ratios.

5. Conclusions

TiAlN/CrN, CrCN/CrN and Mo_2N/CrN multilayer coatings were synthesized using cathodic arc evaporation. The research results can be gathered into three areas:

(1) An analysis of the surface defects. A surface analysis of the coatings formed was carried out, including the determination of the number and size of the coating surface defects and their roughness. It was found that the TiAlN/CrN coating was characterized by the highest roughness Ra, about 0.32 μm, and the Mo_2N/CrN and CrCN/CrN coatings had a similar roughness Ra, slightly below 0.1 μm. The dimensions of the macroparticles were different; most objects were small with dimensions of up to 0.5 μm—about 60%—and up to 1 μm total of about 73%. A few macroparticles which were larger than the thickness of the coating were also observed. The fraction of the sample area covered by the macroparticles increased monotonically with the amount of macroparticles. The melting point of the cathode material directly affected the number and size of the macroparticles and growth-related defects in the coatings. The amount of macroparticles and surface roughness of the coatings increased with the lowering of the melting point of the cathode material. The TiAlN/CrN coating was characterized by a high surface roughness, which was caused by the relatively low melting point intermetallic phase of TiAl.

(2) The mechanical properties of the coatings. The coatings were characterized by a high hardness, with the TiAlN/CrN coating having the lowest, at 21 GPa. The lower hardness of the Ti-based coating compared to the other tested coatings translated into the lowest H/E and H^3/E^2 ratios, suggesting a higher wear among other coatings. These ratios for the Mo-based coating (H = 26 GPa) were similar to those for CrCN/CrN coatings, but despite having the lowest adhesion (Lc = 56 N), they were characterized by the lowest wear rate, 9.0×10^{-8} mm^3/Nm. Coating roughness played an important role here. The titanium coating had more than three times the roughness of the others and this may have been the main reason for the lower wear resistance of these coatings. A phase transformation of $Mo_2N \rightarrow MoO_3$ was also possible. Molybdenum oxide is known as a solid lubricant and can reduce the coefficient of friction and wear rate.

(3) The results of industrial tests. Industrial comparative tests of the coatings showed greater damage to the TiAlN/CrN coating compared to other coatings. Here, as in the case of the other coatings, there was abrasive wear, but also the chipping of the coating layers on the edge of the blade. This chipping, with a thickness of about 200 nm, corresponded to the thickness of a single layer in the coating, rather indicating their weaker cohesion. The rake surface of the tools covered with other coatings showed abrasive wear and there were also only small chippings of the coating on the edge of the blade. This effect could have been associated with the high H/E and H^3/E^2 ratios and/or low surface roughness of the coatings.

Author Contributions: Conceptualization, B.W. and A.G.; methodology, B.W.; software, A.G.; validation, B.W. and A.G.; formal analysis, B.W.; investigation, A.G.; resources, A.G. and M.T.; data curation, A.G. and M.T.; writing—original draft preparation, B.W.; writing—review and editing, B.W. and A.G.; visualization, A.G. and M.T.; supervision, A.G.; project administration, A.G.; funding acquisition, A.G. All authors have read and agreed to the published version of the manuscript.

Funding: This research was funded by the National Center for Research and Development, Poland, grant number BIOSTRATEG3/344303/14/NCBR/2018.

Data Availability Statement: The data presented in this study are available on request from the corresponding author.

Conflicts of Interest: The authors declare no conflict of interest.

References

1. Muhammed, M.; Javidani, M.; Heidari, M.; Jahazi, M. Enhancing the Tribological Performance of Tool Steels for Wood-Processing Applications: A Comprehensive Review. *Metals* **2023**, *13*, 1460. [CrossRef]
2. Warcholinski, B.; Gilewicz, A. Surface Engineering of Woodworking Tools, a Review. *Appl. Sci.* **2022**, *12*, 10389. [CrossRef]
3. Munz, W.D. Titanium aluminum nitride films: A new alternative to TiN coatings. *J. Vac. Sci. Technol. A* **1986**, *4*, 2717–2725. [CrossRef]
4. Kong, Y.; Tian, X.; Gong, C. Enhancement of toughness and wear resistance by CrN/CrCN multilayered coatings for wood processing. *Surf. Coat. Technol.* **2018**, *344*, 204–213. [CrossRef]
5. Adamiak, S.; Bochnowski, W.; Dziedzic, A.; Szyller, Ł.; Adamiak, D. Characteristics of the Structure, Mechanical, and Tribological Properties of a Mo-Mo_2N Nanocomposite Coating Deposited on the Ti6Al4V Alloy by Magnetron Sputtering. *Materials* **2021**, *14*, 6819. [CrossRef]
6. Creasey, S.; Lewis, D.B.; Smith, L.J.; Munz, W.D. SEM image analysis of droplet formation during metal ion etching by a steered arc discharge. *Surf. Coat. Technol.* **1997**, *97*, 163–175. [CrossRef]
7. Munz, W.D.; Smith, L.J.; Lewis, D.B.; Creasey, S. Droplet formation on steel substrates during cathodic steered arc metal ion etching. *Vacuum* **1997**, *48*, 473–481. [CrossRef]
8. Harris, S.G.; Doyle, E.D.; Wong, Y.C.; Munroe, P.R.; Cairney, J.M.; Long, J.M. Reducing the macroparticle content of cathodic arc evaporated TiN coatings. *Surf. Coat. Technol.* **2004**, *183*, 283–294. [CrossRef]
9. Hogmark, S.; Jacobson, S.; Larsson, M. Design and evaluation of tribological coatings. *Wear* **2000**, *246*, 20–33. [CrossRef]
10. Stueber, M.; Holleck, H.; Leiste, H.; Seemann, K.; Ulrich, S.; Ziebert, C. Concepts for the design of advanced nanoscale PVD multilayer protective thin films. *J. Alloys Compd.* **2009**, *483*, 321–333. [CrossRef]
11. Holleck, H.; Schier, V. Multilayer PVD coatings for wear protection. *Surf. Coat. Technol.* **1995**, *76–77*, 328–336. [CrossRef]
12. Santana, A.E.; Karimi, A.; Derflinger, V.H.; Schütze, A. Microstructure and mechanical behavior of TiAlCrN multilayer thin films. *Surf. Coat. Technol.* **2004**, *177–178*, 334–340. [CrossRef]
13. Kot, M.; Rakowski, W.A.; Major, Ł.; Major, R.; Morgiel, J. Effect of bilayer period on properties of Cr/CrN multilayer coatings produced by laser ablation. *Surf. Coat. Technol.* **2008**, *202*, 3501–3506. [CrossRef]
14. Tranca, D.E.; Sobetkii, A.; Hristu, R.; Anton, S.R.; Vasile, E.; Stanciu, S.G.; Banica, C.K.; Fiorentis, E.; Constantinescu, D.; Stanciu, G.A. Structural and Mechanical Properties of CrN Thin Films Deposited on Si Substrate by Using Magnetron Techniques. *Coatings* **2023**, *13*, 219. [CrossRef]
15. Dinu, M.; Mouele, E.S.M.; Parau, A.C.; Vladescu, A.; Petrik, L.F.; Braic, M. Enhancement of the Corrosion Resistance of 304 Stainless Steel by Cr–N and Cr(N,O) Coatings. *Coatings* **2018**, *8*, 132. [CrossRef]
16. Abdallah, B.; Kakhia, M.; Alssadat, W.; Zetoun, W. Study of Power Effect on Structural, Mechanical Properties and Corrosion Behavior of CrN Thin Films Deposited by Magnetron Sputtering. *Prot. Met. Phys. Chem. Surf.* **2021**, *57*, 80–87. [CrossRef]
17. Faga, M.G.; Settineri, L. Innovative anti-wear coatings on cutting tools for wood machining. *Surf. Coat. Technol.* **2006**, *201*, 3002–3007. [CrossRef]
18. Djouadi, M.A.; Nouveau, C.; Beer, P.; Lambertin, M. Cr_xN_y hard coatings deposited with PVD method on tools for wood machining. *Surf. Coat. Technol.* **2000**, *133–134*, 478–483. [CrossRef]
19. Nouveau, C.; Djouadi, M.A.; Decès-Petit, C. The influence of deposition parameters on the wear resistance of Cr_xN_y magnetron sputtering coatings in routing of oriented strand board. *Surf. Coat. Technol.* **2003**, *174–175*, 455–460. [CrossRef]
20. Tritremmel, C.; Daniel, R.; Lechthaler, M.; Polcik, P.; Mitterer, C. Influence of Al and Si content on structure and mechanical properties of arc evaporated Al–Cr–Si–N thin films. *Thin Solid Films* **2013**, *534*, 403–409. [CrossRef]
21. Nouveau, C.; Labidi, C.; Ferreira Martin, J.P.; Collet, R.; Djouadi, M.A. Application of CrAlN coatings on carbide substrates in routing of MDF. *Wear* **2007**, *263*, 1291–1299. [CrossRef]
22. Nadolny, K.; Kapłonek, W.; Sutowska, M.; Sutowski, P.; Myśliński, P.; Gilewicz, A.; Warcholiński, B. Experimental tests of PVD AlCrN-coated planer knives on planing Scots pine (*Pinus sylvestris* L.) under industrial conditions. *Eur. J. Wood Prod.* **2021**, *79*, 645–665. [CrossRef]

23. Benlatreche, Y.; Nouveau, C.; Marchal, R.; Ferreira Martin, J.P.; Aknouche, H. Applications of CrAlN ternary system in wood machining of medium density fibreboard (MDF). *Wear* **2009**, *267*, 1056–1061. [CrossRef]
24. Benlatreche, Y.; Nouveau, C.; Aknouche, H.; Imhoff, L.; Martin, N.; Gavoille, J.; Rousselot, C.; Rauch, Y.J.; Pilloud, D. Physical and Mechanical Properties of CrAlN and CrSiN Ternary Systems for Wood Machining Applications. *Plasma Process. Polym.* **2009**, *6*, S113–S119. [CrossRef]
25. Batista, C.A.; Godoy, C.; Buono, V.T.L.; Matthews, A. Characterisation of duplex (Ti,Al)N and Cr-N PVD coatings. *Mater. Science Eng.* **2002**, *A336*, 39–51. [CrossRef]
26. PalDey, S.; Deevi, S.C. Single layer and multilayer wear resistant coatings of (Ti,Al)N: A review. *Mater. Science Eng.* **2003**, *A342*, 58–79. [CrossRef]
27. Barshilia, H.C.; Prakash, M.S.; Jain, A.; Rajam, K.S. Structure, hardness and thermal stability of TiAlN and nanolayered TiAlN/CrN multilayer films. *Vacuum* **2005**, *77*, 169–179. [CrossRef]
28. Kazmanli, M.K.; Ürgen, M.; Çakir, A.F. Effect of nitrogen pressure, bias voltage and substrate temperature on the phase structure of Mo-N coatings produced by cathodic arc PVD. *Surf. Coat. Technol.* **2003**, *167*, 77–82. [CrossRef]
29. Ürgen, M.; Eryilmaz, O.L.; Çakir, A.F.; Kayali, E.S.; Nilüfer, B.; Işik, Y. Characterization of molybdenum nitride coatings produced by arc-PVD technique. *Surf. Coat. Technol.* **1997**, *94–95*, 501–506. [CrossRef]
30. Sarioglu, S.; Demirler, U.; Kazmanli, M.; Urgen, M. Measurement of residual stresses by X-ray diffraction techniques in MoN and Mo_2N coatings deposited by arc PVD on high-speed steel substrate. *Surf. Coat. Technol.* **2005**, *190*, 238–243. [CrossRef]
31. Gulbiński, W.; Suszko, T. Thin films of MoO_3-Ag_2O binary oxides—The high temperature lubricants. *Wear* **2006**, *261*, 867–873. [CrossRef]
32. Rebholtz, C.; Ziegele, H.; Leyland, A.; Matthews, A. Structure, mechanical and tribological properties of nitrogen-containing chromium coatings prepared by reactive magnetron sputtering. *Surf. Coat. Technol.* **1999**, *115*, 222–229. [CrossRef]
33. Vidakis, S.; Antoniadis, A.; Bilalis, N. The VDI 3198 indentation test evaluation of a reliable qualitative control for layered compounds. *J. Mater. Process. Technol.* **2003**, *143–144*, 481–485. [CrossRef]
34. Romero, J.; Gómez, M.A.; Esteve, J.; Montalà, F.; Carreras, L.; Grifol, M.; Lousa, A. CrAlN coatings deposited by cathodic arc evaporation at different substrate bias. *Thin Solid Films* **2006**, *515*, 113–117. [CrossRef]
35. Stoney, G.G. Tension of metallic films deposited by electrolysis. *Proc. R. Soc. Lond.* **1909**, *A82*, 172–175.
36. Archard, J.F. Contact and rubbing of flat surfaces. *J. Appl. Phys.* **1953**, *24*, 981–988. [CrossRef]
37. Wan, X.S.; Zhao, S.S.; Yang, Y.; Gong, J.; Sun, C. Effects of nitrogen pressure and pulse bias voltage on the properties of Cr-N coatings deposited by arc ion plating. *Surf. Coat. Technol.* **2010**, *204*, 1800–1810. [CrossRef]
38. Warcholinski, B.; Gilewicz, A.; Ratajski, J.; Kuklinski, Z.; Rochowicz, J. An analysis of macroparticle-related defects in the CrCN and CrN coatings in dependence on the substrate bias voltage. *Vacuum* **2012**, *86*, 1235–1239. [CrossRef]
39. Chang, Y.Y.; Yang, S.J.; Wang, D.Y. Structural and mechanical properties of AlTiN/CrN coatings synthesized by a cathodic-arc deposition process. *Surf. Coat. Technol.* **2006**, *201*, 4209–4214. [CrossRef]
40. Chang, Y.Y.; Wang, D.Y.; Hung, C.Y. Structural and mechanical properties of nanolayered TiAlN/CrN coatings synthesized by a cathodic arc deposition process. *Surf. Coat. Technol.* **2005**, *200*, 1702–1708. [CrossRef]
41. Chang, C.L.; Jao, J.Y.; Ho, W.Y.; Wang, D.Y. Influence of bi-layer period thickness on the residual stress, mechanical and tribological properties of nanolayered TiAlN/CrN multi-layer coatings. *Vacuum* **2007**, *81*, 604–609. [CrossRef]
42. Koshy, R.A. Thermally Activated Self-lubricating Nanostructured Coating for Cutting Tool Applications. Ph.D. Thesis, Northwestern University, Evanston, IL, USA, December 2008.
43. Warcholinski, B.; Gilewicz, A. The properties of multilayer CrCN/CrN coatings dependent on their architecture. *Plasma Process. Polym.* **2011**, *8*, 333–339. [CrossRef]
44. Gilewicz, A.; Warcholinski, B. Tribological properties of CrCN/CrN multilayer coatings. *Tribol. Int.* **2014**, *80*, 34–40. [CrossRef]
45. Koshy, R.A.; Graham, M.E.; Marks, L.D. Synthesis and characterization of CrN/Mo_2N multilayers and phases of Molybdenum nitride. *Surf. Coat. Technol.* **2007**, *202*, 1123–1128. [CrossRef]
46. Leyland, A.; Matthews, A. On the significance of the H/E ratio in wear control: A nanocomposite coating approach to optimised tribological behaviour. *Wear* **2000**, *246*, 1–11. [CrossRef]
47. Luo, Q.; Rainforth, W.M.; Münz, W.D. TEM observations of wear mechanisms of TiAlCrN and TiAlN/CrN coatings grown by combined steered-arc/unbalanced magnetron deposition. *Wear* **1999**, *225–229*, 74–82. [CrossRef]
48. Öztürk, A.; Ezirmik, K.V.; Kazmanli, K.; Ürgen, M.; Eryilmaz, O.L.; Erdemir, A. Comparative tribological behaviors of TiN-, CrN- and MoN-Cu nanocomposite coatings. *Tribol. Int.* **2008**, *41*, 49–59. [CrossRef]
49. Erdemir, A. A crystal chemical approach to the lubrication by solids oxides. *Tribol. Lett.* **2000**, *8*, 97–102. [CrossRef]
50. Warcholinski, B.; Gilewicz, A.; Myslinski, P.; Dobruchowska, E.; Murzynski, D.; Kuznetsova, T.A. Effect of Silicon Concentration on the Properties of Al-Cr-Si-N Coatings Deposited Using Cathodic Arc Evaporation. *Materials* **2020**, *13*, 4717. [CrossRef]
51. Gulbiński, W.; Suszko, T.; Sienicki, W.; Warcholiński, B. Tribological properties of silver and copper-doped transition metal oxide coatings. *Wear* **2003**, *254*, 129–135. [CrossRef]
52. Erdemir, A. A crystal chemical approach to the formulation of self-lubricating nanocomposite coatings. *Surf. Coat. Technol.* **2005**, *200*, 1792–1796. [CrossRef]
53. Suszko, T.; Gulbiński, W.; Jagielski, J. The role of surface oxidation in friction processes on molybdenum nitride thin films. *Surf. Coat. Technol.* **2005**, *194*, 319–324. [CrossRef]

54. Solak, N.; Ustel, F.; Urgen, M.; Aydin, S.; Cakir, A.F. Oxidation behavior of molybdenum nitride coatings. *Surf. Coat. Technol.* **2003**, *174–175*, 713–719. [CrossRef]
55. Zhu, X.; Yue, D.; Shang, C.; Fan, M.; Hou, B. Phase composition and tribological performance of molybdenum nitride coatings synthesized by IBAD. *Surf. Coat. Technol.* **2013**, *228*, S184–S189. [CrossRef]